

# geomIO: an open-source MATLAB toolbox to create the initial configuration of 2D/3D thermo-mechanical simulations from 2D vector drawings

Submitted to Geochemistry, Geophysics, Geosystems on November 5, 2018

A. Bauville<sup>1</sup> and T. S. Baumann<sup>2</sup>

<sup>1</sup>Department of Mathematics and Advanced Technology, Japan Agency for Marine-Earth Sciences and Technology, 236-0001 Yokohama, Japan

<sup>2</sup>Johannes Gutenberg University, 55128 Mainz, Germany

## Abstract

Creating the initial geometry and temperature configuration of 3D numerical simulations is a challenging task. Professional tools are expensive. They often have a steep learning curve and do mostly not interface with the numerical simulation software used by the geodynamics and tectonics academic community. There, we developed geomIO (geometry Input/Output), a MATLAB toolbox to create the initial configuration of geological models regarding model geometry and temperature structure. geomIO allows users to create a geo-referenced 3D volume by drawing multiple 2D cross-sections in a standard vector graphics editor. The volume is then used to assign material properties and set up initial temperature distribution on a set of vertices. In 2D mode, polygons can also be used to create a triangular mesh. In addition to the standard functionality, the gravity anomaly of any geometry created with geomIO can be calculated.

In this paper, we give an overview of the basic functionalities of geomIO. We illustrate the strength of our software with advanced tectonic and geodynamic applications that could not have been performed with currently available free software. Applications include the Himalayan orogen, the Japanese subduction zones, present-day salt diapirs, and small-scale tectonic structures. We describe algorithms and file formats in the supporting information.

The toolbox is user-friendly and flexible. Users can use custom pipelines or pre-set data processing pipelines, so most applications require only a few lines of code. geomIO is distributed under the GNU General Public License and includes an online wiki with tutorials and additional examples.

## 1 Introduction

The initial conditions of thermo-mechanical models applied in geology comport two aspects: the geometry of interfaces between rock units, and the temperature distribution. In nature, both of those are non-planar and non-cylindrical, e.g., deformed sedimentary layers in fold-and-thrust belts, subduction geometry, continental blocks in continental collisions.

Commercial software exists that includes geomodeling and numerical simulations tools. However, due to high costs, steep learning curves and lack of flexibility, they are rarely used in the tectonics and geodynamics academic community. Nevertheless, there are many advanced, self-developed simulation software in this community (e.g., i3ELVIS (Gerya and Yuen, 2007), Milamin (Dabrowski et al., 2008), Underworld (Jmansour et al., 2018), LaMEM (Kaus et al., 2016), ASPECT (Kronbichler et al., 2012), pTatin3D (May et al., 2015)). However, adequate tools to design the initial conditions of simulations that easily interface with those codes are still missing.

To answer this problem, we developed the MATLAB toolbox geomIO (geometry Input/Output). The principle of geomIO is to construct 3D geometries from a set of 2D drawings realized in a vector-graphics editor. geomIO processes the vector graphics file and constructs a 2D or 3D geometry. It assigns material phases and adds a temperature distribution to the geometry. Optionally, geomIO can also be used to compute gravity anomalies from this geometry. geomIO was originally developed as a tool to design the initial configuration of the thermo-mechanical 3D simulation code LaMEM (Kaus et al., 2016) for which there is complete compatibility. Furthermore, geomIO is also already partially compatible with the ASPECT software. In 2D, geomIO can construct a body-fitted triangular finite-element mesh or assign properties to vertices for marker-in-cell or particle-based methods.

If required, the user can also construct the geometry in a programming manner. Regardless of the way the 3D geometries were created, the result can be visualized directly in MATLAB or exported to VTK formats, which is why geomIO can also be seen as a general geomodeling tool. Because geomIO saves 3D geometries as polygons on 2D laminae, it natively supports potential field forward modeling, e.g., gravity and magnetic anomaly modeling (Talwani et al., 1959; Talwani and Ewing, 1960).

In this publication, we give an overview of the basic functionalities of geomIO. We illustrate the strength of our software with advanced tectonic and geodynamic applications, that could not have been performed with currently available free software. In the supporting information, we provide a detailed explanation of the algorithms, file formats and an algorithm to interface geomIO with any simulation code. We describe the temperature, topography and phase assignment algorithms, as well as the gravity modeling method. geomIO is developed as open-source software built upon MATLAB and thus provides excellent flexibility to the user and can easily be extended. Links to the online repository and documentation, including additional examples can be found at the official geomIO webpage <https://geomio.bitbucket.io/>.

## 2 Methods

The geomIO toolbox relies on SVG, an XML-based markup language for vector graphics (Bray et al., 2008; Dahlström et al., 2011). geomIO performs five main tasks: (1) SVG files reading and writing; (2) geometry construction and transformations; (3) property assignment to vertices; (4) polygon and temperature file writing; (5) computation of gravity anomalies. geomIO comports pre-set pipelines and options, which allow the user to perform standard data treatment in a single function call. Because geomIO is entirely MATLAB based, it offers the user great flexibility in customizing pipelines and extending functionality. A detailed description of the methods is given in the supporting information, where we describe some additions to the SVG markup language specific to geomIO, the volume construction algorithm, the vertex property mapping algorithms, and the output file formats, and temperature mapping algorithms.

## 3 User interface and examples

geomIO's MATLAB interface comports three basic objects: `geomIO_Options`, `PathCoord` and `Volumes`. `geomIO_Options` is a `class` object that contains information about the SVG file, coordinate system, and various options for the data treatment and output. `PathCoord` is a `struct` object that stores information about the shapes drawn, such as coordinates, style (color, stroke, etc.), phase, label, etc. It stores information both about the SVG shapes (Bezier curve, ellipse, or rectangle) and the polygon created from these by geomIO (i.e., discretized bezier curve, ellipse, etc.). `Volumes` is a `struct` object that stores the polyhedrons, including coordinate of polyhedron vertices, triangulation map, and phase.

In the folder `Tutorials`, we included a variety of SVG files and matlab scripts to perform basic and advanced tasks with `geomIO`, and reproduce some of the results presented here. The tutorials and examples cover basic 2D (Fig. 1A) and 3D usage (Fig. 2), 2D triangulation (Fig. 1B), 3D geodynamic model (Fig. S2), 3D temperature distribution around a slab (Fig. 6) and 2D/3D Gravity (Fig. S3)

### 3.1 Installation

The `geomIO` website (<https://geomio.bitbucket.io/>) provides links to the git-repository and documentation. To install the `geomIO-toolbox`, users must clone the repository and include the source directory into the MATLAB path by running the `install_geomIO` script.

### 3.2 Tutorial 1: Constructing a 2D geometry

In this first example, we use Inkscape (<https://inkscape.org>) and `geomIO` to create the phase distribution of a 2D simulation (Fig. 1). First, we open Inkscape, draw one shape, and save it as an "Inkscape SVG" file (default file format). We open the XML editor and add new attributes to assign a phase number (not optional, although it can be (re-)assigned from within a `geomIO` program) and a label (optional in 2D) to the particular shape (e.g. a `<path>`). New attributes can be created by adding a name and value to the attribute name and value fields, respectively. The second step is performed in MATLAB. Here, we assign the given phase to vertices inside the drawn shape (polygon). A script example is given below.

```
% 1. Read paths from the svg file
% =====
opt          = geomIO_Options();
opt.inputFileName = ['./Input/mySvgFile.svg'];
[PathCoord]   = run_geomIO(opt, '2D');

% 2. Create vertices to which to assign phases
% =====
xmin = 0; xmax = opt.svg.width;
ymin = 0; ymax = opt.svg.height;
[Xp, Yp] = ndgrid(xmin:15:xmax, ymin:15:ymax);
Phase    = zeros(size(Xp));

% 3. Assign a phase to vertices
% =====
Phase = assignPhase2Markers(PathCoord, opt, Xp, Yp, Phase);
```

The script comports three steps:

1. A set of default values is assigned to `opt`. In this example, only `opt.inputFileName` is specified; all other options remain at their default value. The `run_geomIO` function contains preset data treatment pipelines and returns a `PathCoord` and/or a `Volumes` object. Here, we used the '2D' pipeline.
2. We create a set of three matrices containing X, Y coordinates and a phase number for all vertices. Here, we use the 'paper sheet' from the SVG file as model space, such that the model space and drawing space have the same coordinates. A different model space coordinate system can be specified by adding a 'Reference' layer to the SVG file as shown in the next example.
3. We attribute a phase number to vertices.

## 2D mode

### vector drawing

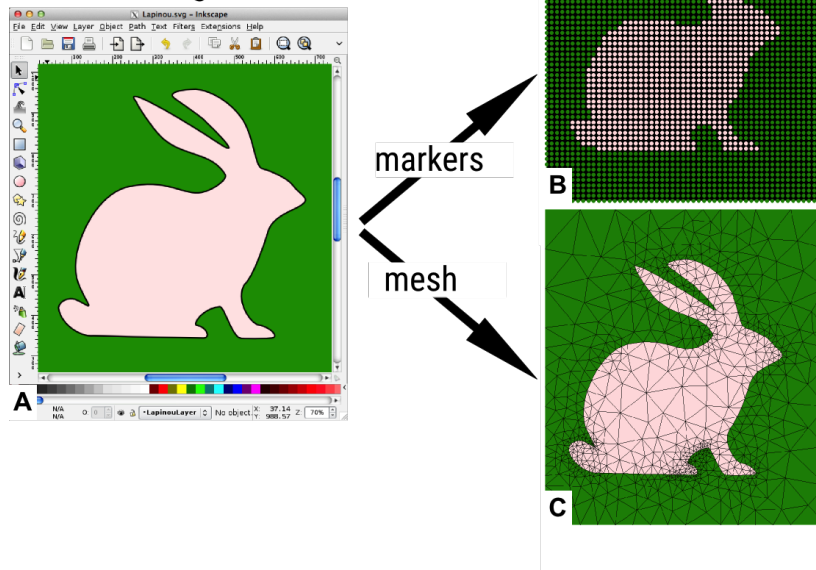


Figure 1: geomIO's basic 2D functionality. **A)** The Inkscape environment (i.e. drawing space). **B)** Markers assigned inside the model space according to the drawn polygon. **C)** Alternatively, a triangular mesh can be generated.

Tutorials and program examples to generate triangular mesh (Fig. 1.C) and handling multiple polygons are available in the `Tutorials` folder.

### 3.3 Tutorial 2: Constructing a 3D geometry

#### 3.3.1 Inkscape walkthrough example

The second example illustrates the creation of phase and temperature initial conditions for a 3D simulation (Fig. 2). First, we open Inkscape, draw one shape, add a label and a phase to this shape and save it as an 'Inkscape SVG' file (Figure 2 A). The name of the file should follow the format `myfilename.OR.svg`, where `OR` indicates the orientation of the drawing plane in the model space and is either `HZ`, `NS` or `EW`, respectively, horizontal, North-South or East-West vertical plane.

Second, we create a new layer. Layer names indicate the coordinate in the direction normal to the drawing plane. The layer name follows the format `letter numbers`, without space, dots or commas. The letter indicates the sign, `+` (`p`) or `-` (`m`) and the number indicates the position along the axis perpendicular to the drawing plane, (i.e. `p0030` (30), `m250` (-250)). Values must be given in the units used for the model space. `p` also denotes the decimal separator, i.e. `m3p55` corresponds to a value of -3.55 of the respective unit. Additional layers, starting with a `#` sign can also be used for reference and will not be processed by geomIO. One may want to add images in the file. In such case, the user should link the images rather than embed them.

Third, we duplicate the first shape (`Ctrl+d/Cmd+d`) and transfer it to another layer (Figure 2 B). Without adding new points, we move the points defining the first shape to fit another shape. This constraint is required by the meshing algorithm and is based on animation methods (Parke, 1972). A more detailed description is given in the supporting information.

The default background phase is 0. To specify a non-default value, another shape covering the whole domain can be added to each layer. This layer should be given a label and a phase. When several shapes with different phases are superposed on the same layer,

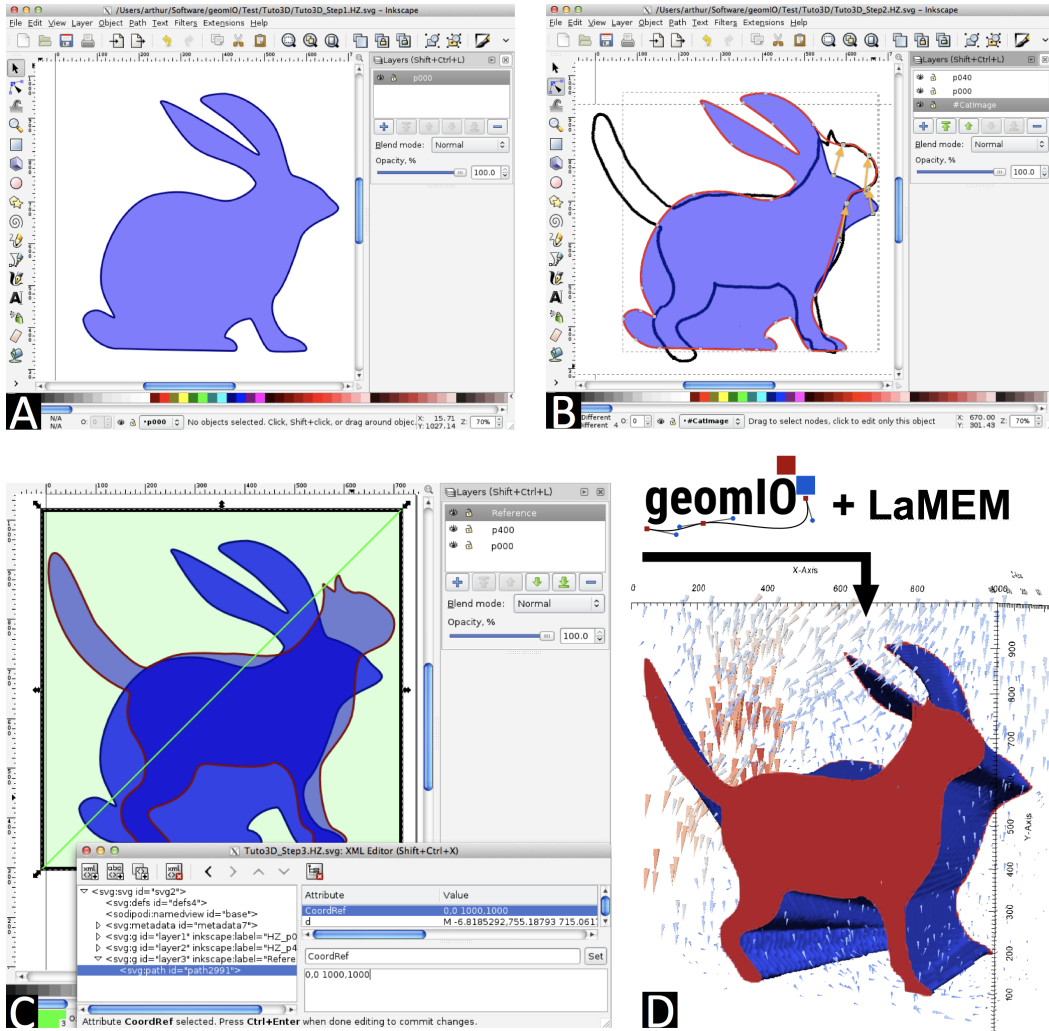


Figure 2: Creation process of a numerical simulation's initial geometry. **A)** Drawing a first shape in Inkscape. **B)** Duplicate this shape to a different layer and create a new shape by displacing the control points that defined the first shape. **C)** Adding a 'Reference' layer to specify coordinate transformations between the drawing and model space. **D)** From the SVG file, geomIO has created a polyhedron which is used as the initial condition for a numerical simulation using LaMEM (Kaus et al., 2016)

geomIO assigns phases from the bottom to the top shape, i.e., in the same manner that Inkscape draws shapes to the screen.

A special layer called Reference can also be added (Figure 2 D). This layer must contain only one path: a line that defines the coordinate transformation from the drawing coordinate system to the model coordinate system. This line only defines translation and scaling transformation. It does not need a label but requires a special attribute CoordRef with values:  $x_1, y_1 \ x_2, y_2$ , where  $x$  and  $y$  denote the coordinates of the line segment in the model coordinate system.

### 3.3.2 MATLAB walkthrough example

Once the drawing phase is done, the user should start a MATLAB session. The following script demonstrates how to read the file and create the associated polyhedron.

```
opt = geomIO_Options();
opt.inputFileName = ['Test.HZ.svg'];
[PathCoord, Volumes] = run_geomIO(opt);
```

Polyhedrons/volumes can be visualized in MATLAB with the function `plotVolumes(Volumes)`. geomIO can also output VTK files. By default, these files are written in the directory `./Output/`. For optimal visualization one can slightly shift the volumes, such that they do not overlap using the option `opt.shiftPVobj = [dx dy dz]`. The 'Polygon' file format described in the supporting information allows the user to transfer geomIO's polyhedron into a numerical simulation software. A polygon file can be written by setting the option `opt.writePolygons = true`. The modified code looks like:

```
opt = geomIO_Options();
opt.inputFileName = ['Test.HZ.svg'];
opt.writeParaview = true;
opt.shiftPVobj = [0 0 1];
opt.writePolygons = true;
[PathCoord, Volumes] = run_geomIO(opt);
```

### 3.3.3 Topography and temperature

Geodynamic applications often require setting a topography and temperature distribution. The function `initTopo` constructs a topography grid based on previously created volumes. The function `initTemp` allows the user to apply vertical temperature profiles based on the shapes drawn at the surface of the model. An example of constructing such a model is given in `/tutorials/Example3D_Geodynamics`. The topography and temperature output of this example is shown in Supplementary Fig. S2.

## 4 Applications

In this section, we present four applications that illustrate advanced capabilities of geomIO.

### 4.1 2D: Small scale structure mechanics based on a photograph

The first application illustrates a way of studying the mechanics of small-scale geological structures from a photograph using Inkscape's automatic vectorization functionality. First, we selected a picture of a small scale geological structure, here a set of en-echelon veins (Figure 3 A). The Trace bitmap functionality of Inkscape automatically created a set of paths capturing the outline of the structures (Figure 3 B).

In a second step, we used geomIO to read the SVG file. The set of created Polygons is stored in PathCoord from which it was extracted and passed to the mesh generator

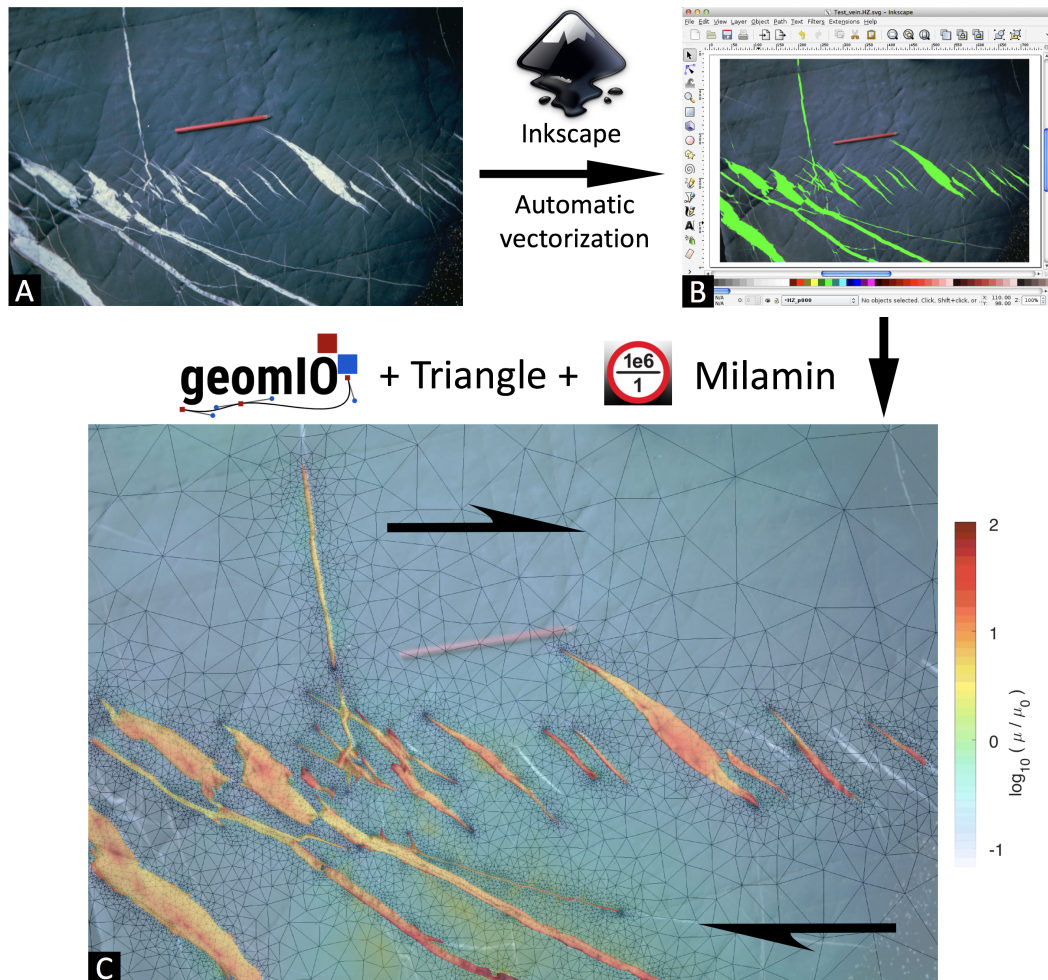


Figure 3: By combining Inkscape's automatic vectorization functionality with geomIO and Triangle (Shewchuk, 1996) a triangular finite element mesh can easily be created from a picture. **A)** Picture of en-echelon veins (picture by John Ramsay, courtesy of Mark Brandon). **B)** Vectorized image. **C)** We used geomIO to extract polygons from the SVG file containing the vectorized image. Polygons were then passed as input for Triangle to create a triangular mesh. We assigned material properties and performed a mechanical numerical simulation to compute the value of non-linear viscosity  $\mu$ .

*Triangle* (Shewchuk, 1996). We attributed a given phase to elements within the polygons and a different one to the matrix surrounding them. Finally, we performed a numerical simulation using the mesh as an input for MILAMIN (Dabrowski et al., 2008). MILAMIN solves the equations of Stokes which describe the flow of rocks at geological timescales. For the simulation presented in Figure 3 C, the rheology in the model is non-linear viscous with a stress exponent of five, and the reference viscosity  $\mu_0$  of the veins is ten times higher than that of the matrix.

## 4.2 3D: Creating a present-day model of the India-Asia orogen

The second application is related to a project aiming at constraining the rheological properties of the main geological units of the Himalayas by inversion methods (Baumann, 2016). The Himalayas are composed of many tectonic units of contrasting rheology and therefore the accuracy of the inversion results also depend on the quality of the geometrical model (Fig. 4). *geomIO* allowed us to build a very detailed model of the region. Baumann (2016) created a set of images using GMT (Wessel and Smith, 1998). These images contain relevant data and geophysical models from which we interpreted the geometry of the main geological units (Fig. 4A and B). The data includes five different seismological records. An SV-wave tomography by Schaeffer and Lebedev (2013) is used as the basis of the model. Baumann (2016) also analysed 24 receiver function (RF) profiles in the region to collect complementary information on the depths of the Lithosphere Asthenosphere boundary (LAB) and the Moho (Zhang et al., 2014; Xu et al., 2014; Mechie and Kind, 2013; Schneider et al., 2013; Sippl et al., 2013; Zhao et al., 2010; Nábelek et al., 2009; Kumar et al., 2006; Rai et al., 2006; Schulte-Pelkum et al., 2005; Wittlinger et al., 2004; Vergne et al., 2002). The Moho signals of these profiles can be seen as a refinement of the Crust 1.0 model (Laske et al., 2013), which is also included in our joint interpretation. The Crust 1.0 model has a  $1^\circ \times 1^\circ$  resolution. Therefore, the interpretation mostly followed local studies when available. For the interpretation of transform plate boundaries and subduction zones, we took into account the seismicity distribution and focal solutions (Ekström et al., 2012; Dziewonski et al., 1981). (Baumann, 2016) also extracted additional information from teleseismic tomography (He et al., 2010) and seismic reflection studies (Gao et al., 2013). All locations and orientations of these studies incorporated in the model geometry are marked in Fig.4A.

We automatically created an SVG file containing all the images in independent layers using *geomIO*'s `writeSVG` function with options `opt.imgAdd = True` and `opt.imgDir = "./imageDirector` where `opt.imgDir` contains the address of a directory containing images whose names correspond to the layers that contain said images in the SVG file. The interpretation of the geological units was conducted on individual layers using Inkscape. We drew the contours of particular units on different cross-sections following the rules described in section 3.3.

These steps were repeated for NS-, EW- and horizontal cross-sections. We projected the contours drawn in one section to the other sections and integrated them into new SVG files. For example, after drawing contours in NS cross-sections and creating a `Volumes-object`, we obtained polygons in EW cross-section by calling the function `makePolygonSlices` for this `Volumes-object`. The polygons thus created can be integrated into a new `PathCoord` object, and used as input to the `writeSVG` function, which generates a new SVG file containing the projection of the contours.

Figure 4C shows the final set of polyhedrons which we used as input to LaMEM. Despite the complexity of the geometric model, the interpretation of the geometry can easily be reviewed and discussed since it is built from a set of 2D sections. This simplifies collaborations and the peer review process. A model created with *geomIO* reduces the biases from artifacts of individual geophysical and geological methods as it combines the interpretation of multiple, independent data sources.



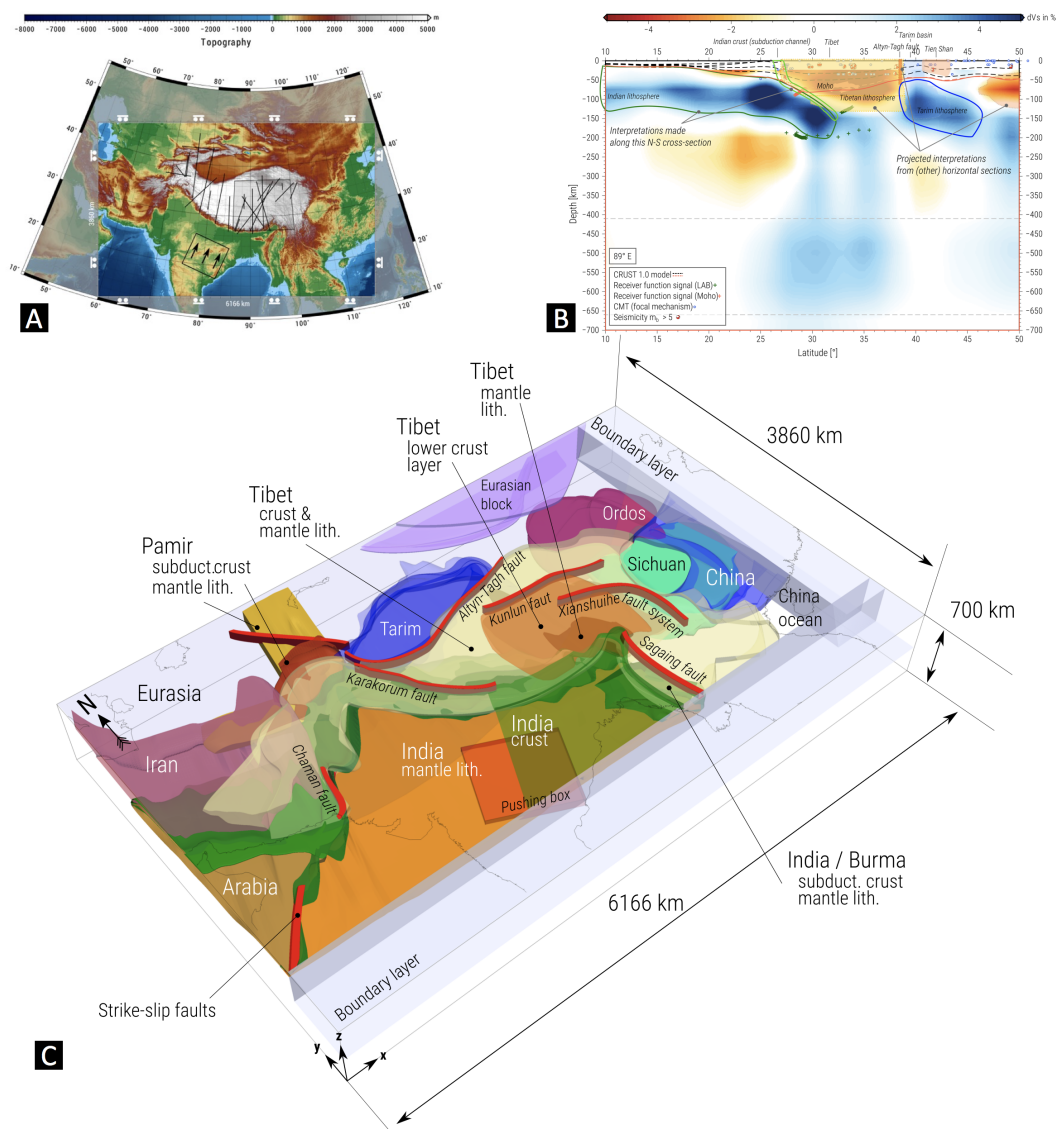


Figure 4: Constructing a 3D model with the main geological regions of the Himalayas and the Tibetan plateau. **A)** Geographical setting. The clear region of the map represents the model space. The ‘rollers’ symbol indicates free-slip boundary conditions. In the box over India, the observed velocity is imposed in the direction of the arrows. Lines indicate the location of the receiver function studies used to construct the geometry. **B)** Example of an NS-oriented cross-section showing geophysical constraints and orthographic interpretations. The cross-sections contain a seismic tomographic model, the crust 1.0 model and the hypocenters of major earthquakes as well as Moho and LAB depths from receiver function studies. All of these data were used as a reference to construct the geometry. **C)** The final set of polyhedrons visualized. Colors indicate major geological units.

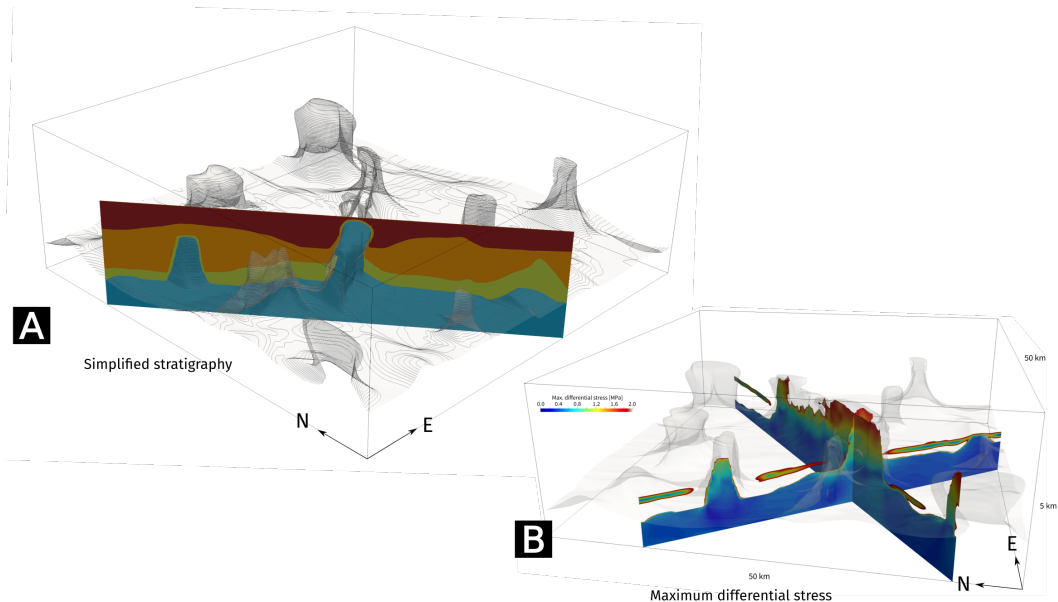


Figure 5: **A)** Model geometry of 3D salt structures. Available stratigraphic data of the overburden geology was extracted from online map servers (GEOTIS Agemar et al. (2014), and NIBIS Landesamt für Bergbau (2014)) **B)** Example simulation result showing the maximum differential stress visualized only inside the salt structures.

### 4.3 Salt structure

Another application is demonstrated in Fig. 5. Here, we collected all available data to build a present-day 3D model geometry and compute stresses and strain rates within and around salt structures in Northern Germany (Baumann et al., 2018). We used stratigraphic data available from the online map servers (GEOTIS (Agemar et al., 2014), NIBIS (Landesamt für Bergbau, 2014)). These web tools offer the possibility to project map data on cross-sections. After gathering and interpreting data on many vertical cross-sections, we used geomIO to merge and compile data into a 3D model.

### 4.4 Temperature profile for the slabs in Japan

For this application, we constructed a temperature distribution for the Japan subduction zone (Fig. 6), based on the slab geometry and estimates of the plate's age. We used two SVG files to draw the Pacific and Philippine sea plate separately and merged them into the same Volumes in MATLAB. We constructed an approximate Voronoi diagram to obtain the distance from the slab for a vertices of a 3D grid. Using the distance information, we set the temperature distribution using a half-space cooling model with age of 50 Ma, 20 Ma, and 150 Ma for the Eurasian/North-American plate, Philippine sea slab and Pacific slab respectively. Constructing slab geometry and temperature distribution is challenging (e.g., Hayes et al., 2012; Jadamec and Billen, 2012), but with geomIO and using age maps (Müller et al., 2008) the process is relatively straightforward and easy to perform. The temperature distribution of this application can be created by running `/tutorials/Example3D_Slab_Temperature/Main_geomIO.m`.

## 5 Summary

geomIO is a MATLAB toolbox that allows its users to easily create a 3D geometry and temperature distribution based on a series of 2D vector drawings. With geomIO, we aim to support researchers in the field of geodynamics and tectonics to create complex initial

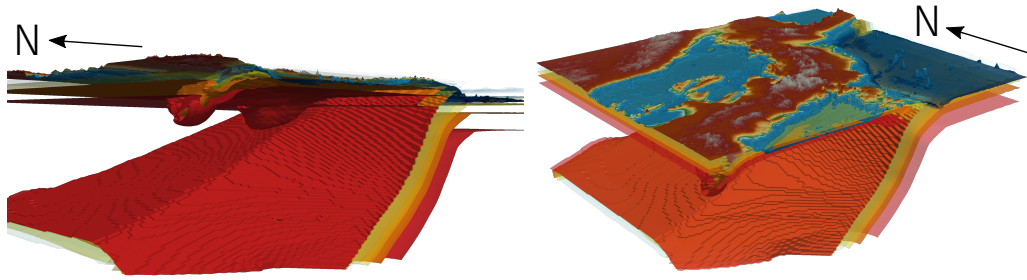


Figure 6: Two perspectives of the temperature structure in the Japanese subduction zone, constructed with geomIO. The slab geometry is based on the work by Hasegawa et al. (2009) and the temperature was assigned according to a half-space cooling model below the slabs' surface.

configurations of thermo-mechanical simulations to improve the accuracy and reliability of forward and inverse simulations of geological phenomena.

For the construction of geometries, we rely on open source software for vector graphics. In the academic geodynamics community, geomIO's 3D functionality is currently supported by LaMEM. 2D features are also supported by ASPECT. The accompanying supplements and the online repository provide templates for integrating geomIO input into other 3D thermomechanical codes. How to use geomIO inputs with any MATLAB based software is fully described and supported with online examples.

This paper describes the basic strategy and underlying algorithms of geomIO. We show detailed solutions to simple tasks and describe the advanced features of the software through applications of simple cases and complex geometrical models and temperature distributions.

## Acknowledgments

This work was supported by the European Research Council under the European Community's Seventh Framework program (FP7/2007/2013) with ERC starting Grant Agreement No. 258830 and the SNF early PostDoc.Mobility Grant No. 161927. We are grateful to Dave May and an anonymous reviewer for their constructive comments and suggestions which helped improving the quality of this paper as well as the quality of the software and its documentation. geomIO is free software distributed under the Creative Commons license. Online resources can be found at <https://geomio.bitbucket.io/>. geomIO includes the open source functions 'intersectPlaneSurf' by Ozturk (2014), 'inpoly' by Redish and Jaquetot (2008) and 'PetscBinaryWrite' by Balay et al. (2018).

## References

- Agemar, T., Alten, J.-A., Ganz, B., Kuder, J., Kühne, K., Schumacher, S., and Schulz, R. (2014). The geothermal information system for germany–geotis. *Zeitschrift der deutschen Gesellschaft für Geowissenschaften*, 165(2):129–144.
- Balay, S., Abhyankar, S., Adams, M. F., Brown, J., Brune, P., Buschelman, K., Dalcin, L., Dener, A., Eijkhout, V., Gropp, W. D., Kaushik, D., Knepley, M. G., May, D. A., McInnes, L. C., Mills, R. T., Munson, T., Rupp, K., Sanan, P., Smith, B. F., Zampini, S., Zhang, H., and Zhang, H. (2018). PETSc users manual. Technical Report ANL-95/11 - Revision 3.10, Argonne National Laboratory.
- Baumann, T. S. (2016). *Geodynamic Inversion to Constrain the Rheology of the Lithosphere*. PhD thesis, Universitätsbibliothek Mainz.

- Baumann, T. S., Kaus, B. J., and Popov, A. A. (2018). Deformation and stresses related to the gorleben salt structure: insights from 3d numerical models. In *Mechanical Behavior of Salt, Saltmech IX, 2018, Hannover*, pages 15–27.
- Bray, T., Paoli, J., Sperberg-McQueen, C., and Maler, E. (2008). *Extensible markup language (XML) 1.0*.
- Dabrowski, M., Krotkiewski, M., and Schmid, D. W. (2008). MILAMIN: MATLAB-based finite element method solver for large problems. *Geochemistry, Geophysics, Geosystems*, 9(4).
- Dahlström, E., Dengler, P., Grasso, A., and Lilley, C. (2011). Scalable vector graphics (svg) 1.1. *World Wide Web*.
- Dziewonski, A. M., Chou, T.-A., and Woodhouse, J. H. (1981). Determination of earthquake source parameters from waveform data for studies of global and regional seismicity. *J. Geophys. Res. Solid Earth*, 86(B4):2825–2852.
- Ekström, G., Nettles, M., and Dziewoński, A. (2012). The global cmt project 2004–2010: centroid-moment tensors for 13,017 earthquakes. *Phys. Earth Planet. In.*, 200:1–9.
- Gao, R., Chen, C., Lu, Z., Brown, L. D., Xiong, X., Li, W., and Deng, G. (2013). New constraints on crustal structure and Moho topography in Central Tibet revealed by SinoProbe deep seismic reflection profiling. *Tectonophysics*, 606:160–170.
- Gerya, T. V. and Yuen, D. A. (2007). Robust characteristics method for modelling multiphase visco-elasto-plastic thermo-mechanical problems. *Physics of the Earth and Planetary Interiors*, 163(1-4):83–105.
- Hasegawa, A., Nakajima, J., Uchida, N., Okada, T., Zhao, D., Matsuzawa, T., and Umino, N. (2009). Plate subduction, and generation of earthquakes and magmas in japan as inferred from seismic observations: an overview. *Gondwana Research*, 16(3-4):370–400.
- Hayes, G. P., Wald, D. J., and Johnson, R. L. (2012). Slab1. 0: A three-dimensional model of global subduction zone geometries. *Journal of Geophysical Research: Solid Earth*, 117(B1).
- He, R., Zhao, D., Gao, R., and Zheng, H. (2010). Tracing the Indian lithospheric mantle beneath central Tibetan Plateau using teleseismic tomography. *Tectonophysics*, 491(1-4):230–243.
- Jadamec, M. A. and Billen, M. I. (2012). The role of rheology and slab shape on rapid mantle flow: Three-dimensional numerical models of the Alaska slab edge. *J. Geophys. Res.*, 117.
- Jmansour, Kaluza, O., Giordani, J., Rbeucher, RebeccaFarrington, Kennedy, G., Moresi, L., , M., Adambeall, and Sandiford, D. (2018). Underworldcode/underworld2: V2.6.0b.
- Kaus, B. J. P., Popov, A. A., Baumann, T. S., U Ok, A. E., Bauville, A., Fernandez, N., Collignon, M., Kaus, B. J. P., Popov, A. A., Baumann, T. S., Usök, A. E., Bauville, A., Fernandez, N., and Collignon, M. (2016). Forward and Inverse Modelling of Lithospheric Deformation on Geological Timescales. *NIC Series*, 48:978–3.
- Kronbichler, M., Heister, T., and Bangerth, W. (2012). High accuracy mantle convection simulation through modern numerical methods. *Geophysical Journal International*, 191(1):12–29.

- Kumar, P., Yuan, X., Kind, R., and Ni, J. (2006). Imaging the colliding Indian and Asian lithospheric plates beneath Tibet. *J. Geophys. Res.*, 111(B6):B06308.
- Landesamt für Bergbau, Energie und Geologie (LBEG), H. (2014). Nibis® kartenserver: Nibis® kartenserver.
- Laske, G., Masters, G., Ma, Z., and Pasyanos, M. (2013). Update on CRUST1.0 - A 1-degree global model of Earth's crust. In *Geophys. Res. Abstr.*, number EGU2013-2658 in 15.
- May, D., Brown, J., and Pourhiet, L. L. (2015). A scalable, matrix-free multigrid preconditioner for finite element discretizations of heterogeneous Stokes flow. *Computer Methods in Applied Mechanics and Engineering*, 290:496 – 523.
- Mechie, J. and Kind, R. (2013). A model of the crust and mantle structure down to 700km depth beneath the Lhasa to Golmud transect across the Tibetan plateau as derived from seismological data. *Tectonophysics*, 606:187–197.
- Müller, R. D., Sdrolias, M., Gaina, C., and Roest, W. R. (2008). Age, spreading rates, and spreading asymmetry of the world's ocean crust. *Geochemistry, Geophysics, Geosystems*, 9(4).
- Nábelek, J., Hetényi, G., Vergne, J., Sapkota, S., Kafle, B., Jiang, M., Su, H., Chen, J., and Huang, B.-S. (2009). Underplating in the Himalaya-Tibet collision zone revealed by the Hi-CLIMB experiment. *Science*, 325(5946):1371–4.
- Ozturk, M. (2014). intersectPlaneSurf. MATLAB Central File Exchange. Retrieved March 25, 2015. <https://www.mathworks.com/matlabcentral/fileexchange/intersectPlaneSurf>.
- Parke, F. (1972). Computer generated animation of faces. *Proceedings of the ACM annual conference-Volume 1*.
- Rai, S. S., Priestley, K., Gaur, V. K., Mitra, S., Singh, M. P., and Searle, M. (2006). Configuration of the Indian Moho beneath the NW Himalaya and Ladakh. *Geophys. Res. Lett.*, 33(15):L15308.
- Redish, A. D. and Jaquenot, G. (2008). Fast InPolygon detection MEX. MATLAB Central File Exchange. Retrieved May 15, 2015. <https://www.mathworks.com/matlabcentral/fileexchange/Fast-InPolygon-detection-MEX>.
- Schaeffer, A. J. and Lebedev, S. (2013). Global shear speed structure of the upper mantle and transition zone. *Geophys. J. Int.*, 194(1):417–449.
- Schneider, F., Yuan, X., Schurr, B., Mechie, J., Sippl, C., Haberland, C., Minaev, V., Oimahmadov, I., Gadoev, M., Radjabov, N., Abdybachaev, U., Orunbaev, S., and Negmatullaev, S. (2013). Seismic imaging of subducting continental lower crust beneath the Pamir. *Earth Planet. Sci. Lett.*, 375:101–112.
- Schulte-Pelkum, V., Monsalve, G., Sheehan, A., Pandey, M. R., Sapkota, S., Bilham, R., and Wu, F. (2005). Imaging the Indian subcontinent beneath the Himalaya. *Nature*, 435(7046):1222–5.
- Shewchuk, J. R. (1996). Triangle: Engineering a 2D quality mesh generator and Delaunay triangulator. pages 203–222. Springer, Berlin, Heidelberg.
- Sipl, C., Schurr, B., Tymphel, J., Angiboust, S., Mechie, J., Yuan, X., Schneider, F., Sobolev, S., Ratschbacher, L., and Haberland, C. (2013). Deep burial of Asian continental crust beneath the Pamir imaged with local earthquake tomography. *Earth Planet. Sci. Lett.*, 384:165–177.

- Talwani, M. and Ewing, M. (1960). Rapid computation of gravitational attraction of three-dimensional bodies of arbitrary shape. *Geophysics*, 25(1):203–225.
- Talwani, M., Worzel, J. L., and Landisman, M. (1959). Rapid gravity computations for two-dimensional bodies with application to the mendocino submarine fracture zone. *Journal of geophysical research*, 64(1):49–59.
- Turcotte, D. and Schubert, G. (2014). *Geodynamics*. Cambridge University Press, Cambridge, third edition.
- Velić, M., May, D., and Moresi, L. (2009). A Fast Robust Algorithm for Computing Discrete Voronoi Diagrams. *Journal of Mathematical Modelling and Algorithms*, 8(3):343–355.
- Vergne, J., Wittlinger, G., Hui, Q., Tapponnier, P., Poupinet, G., Mei, J., Herquel, G., and Paul, A. (2002). Seismic evidence for stepwise thickening of the crust across the NE Tibetan plateau. *Earth Planet. Sci. Lett.*, 203(1):25–33.
- Wessel, P. and Smith, W. (1998). New, improved version of Generic Mapping Tools released. *Eos, Transactions American*.
- Wittlinger, G., Vergne, J., Tapponnier, P., Farra, V., Poupinet, G., Jiang, M., Su, H., Herquel, G., and Paul, A. (2004). Teleseismic imaging of subducting lithosphere and Moho offsets beneath western Tibet. *Earth Planet. Sci. Lett.*, 221(1-4):117–130.
- Xu, T., Wu, Z., Zhang, Z., Tian, X., Deng, Y., Wu, C., and Teng, J. (2014). Crustal structure across the Kunlun fault from passive source seismic profiling in East Tibet. *Tectonophysics*, 627:98–107.
- Zhang, Z., Wang, Y., Houseman, G. a., Xu, T., Wu, Z., Yuan, X., Chen, Y., Tian, X., Bai, Z., and Teng, J. (2014). The Moho beneath western Tibet: Shear zones and eclogitization in the lower crust. *Earth Planet. Sci. Lett.*, 408:370–377.
- Zhao, J., Yuan, X., Liu, H., Kumar, P., Pei, S., Kind, R., Zhang, Z., Teng, J., Ding, L., and Gao, X. (2010). The boundary between the Indian and Asian tectonic plates below Tibet. *Proc. Natl. Acad. Sci.*, 107(25):11229–11233.

## Supporting information

### S1. Introduction

In this supplementary material, we describe original algorithms and data format used by geomIO. We describe some additions to the SVG markup language specific to geomIO, the volume construction algorithm, vertex property mapping algorithms for material phase and temperature. We also describe the output file formats and the gravity computation algorithm.

### S2. A brief overview of the SVG file format and its usage in geomIO

SVG is an XML-based markup language and file format to describe two-dimensional graphics (Bray et al., 2008; Dahlström et al., 2011). As XML files, SVG images can be created and edited with any text editor, or with specialized drawing software. SVG allows for three types of graphic objects: vector graphic shapes (e.g., paths consisting of straight lines and curves), images and text. In geomIO, we make use of the vector graphic shape objects only. Users can also use images and text during the design of their model, but the software performs no data treatment on them.

The SVG file format allows some latitude in syntax, and each vector graphics editor has slight differences in their choice of syntax, which makes handling of arbitrary vector graphics editor difficult. Due to the design of geomIO, we recommend using a graphics editor, which allows editing the text file directly. Currently, geomIO is tested and optimized for the latest stable version of Inkscape (v0.92), a popular free cross-platform open-source vector-graphics editor available for Windows, Linux, and Mac OS. geomIO partially supports Adobe Illustrator but many functions are missing, and we have not performed extensive testing. Consequently, we do recommend to use Inkscape (v0.92) with geomIO. An SVG file created with Inkscape typically looks like the following:

```
<?xml version="1.0" encoding="UTF-8" standalone="no"?>
<svg
  document formatting and file info>
  <g
    inkscape:label="Layer 1"
    inkscape:groupmode="layer"
    id="layer1">
    <path
      style="A character string with style information"
      d="m 311.42857,269.50506 c 0,0 -131.42857,71.42857 -57.14286,114.28572"
      id="path4136"
    />
  </g>
</svg>
```

The tag `<svg>` stores all document information, the `<g>` tag stores information related to a given layer and `<path>` stores information of a drawn path (i.e., a polygon created from Bezier curves). Inside `<path>` the attribute `d` stores the data needed to construct the path and `id` denotes the unique name of a given object. The full description of the SVG format can be found in Dahlström et al. (2011).

In geomIO we add two more attributes to layers (`<g>`) and geometry objects (`<path>`, `<line>`, `<ellipse>`). The first one, `label="myLabel"`, is used to group polygons that are scattered across several layers and will be used to construct a single volume. The second

Table S1. Special layers and attributes

Label	Content	Attribute	Description
Reference	<line> or <path>	CoordRef="x1,y1,x2,y2"	Contains a single line or path with the added attribute CoordRef. Used to make coordinate transformation from the drawing to the model space.
Box	<rect>	none	Contains a single rectangle whose coordinate define the limits of the model domain.
#Label	any	none	Layers whose label start with ""#" are not processed. They can be used to add notes or information that helps the original design. Pasted images should be added to these layers.

one, phase="1", contains a number indicating the material phase that will be attributed to particles or elements inside the drawn path. Additionally, some of the layers have specific labels with a particular meaning in geomIO. They are described in Table ??.

### S3. Polyhedron construction algorithm

We start defining the model space with coordinates  $x, y, z$  and the drawing space with coordinates  $\bar{x}, \bar{y}, \bar{z}$ . The model space is the ‘target’ space, where the volume will be used. For example, it can be the space of a numerical simulation or the one of the geo-referenced volume. The drawing space is where volume slices are drawn. The drawing plane in Inkscape, i.e., the coordinate frame in the SVG file, is the plane defined by  $\bar{x}$  and  $\bar{y}$ . Individual slices of a volume are parallel and distributed along the  $\bar{z}$  direction. If the model space is Cartesian then coordinates can be transformed from the drawing to the model space by applying translation and scaling transformations:

$$\begin{pmatrix} x \\ y \\ z \\ 1 \end{pmatrix} = \begin{pmatrix} \alpha_x & 0 & 0 & \Delta_x \\ 0 & \alpha_y & 0 & \Delta_y \\ 0 & 0 & \alpha_z & \Delta_z \end{pmatrix} \cdot \begin{pmatrix} \bar{x} \\ \bar{y} \\ \bar{z} \\ 1 \end{pmatrix}, \quad (1)$$

where  $\alpha_x, \alpha_y, \alpha_z$  are scaling factors and  $\Delta_x, \Delta_y, \Delta_z$  are translation factors. By default, the drawing plane is assumed to correspond to either the E-W, N-S, or horizontal plane. This nomenclature refers to the orientation in a Cartesian coordinate system rather than geographic coordinates. If drawings are performed in one of those three directions geomIO will correctly position volumes drawn in different orientations. Other orientations can be used but require the user to apply a rotation to eq. 1.

In geomIO, a polyhedron (3D volume) is constructed from a series of parallel polygons (2D surface). In the following, we will use the terms ‘polyhedron’ and ‘volume’ interchangeably. Each polygon is defined in the  $\bar{x}, \bar{y}$  space at a given position along  $\bar{z}$ . Each polygon from which a polyhedron will be constructed must include the same number of vertices. This constraint has two advantages. First, it allows a simple and robust triangular meshing of the polyhedron surface by connecting nodes with the same index across the different slices. Second, it permits the creation of intermediate slices by interpolating the position of a given node along  $\bar{z}$ .



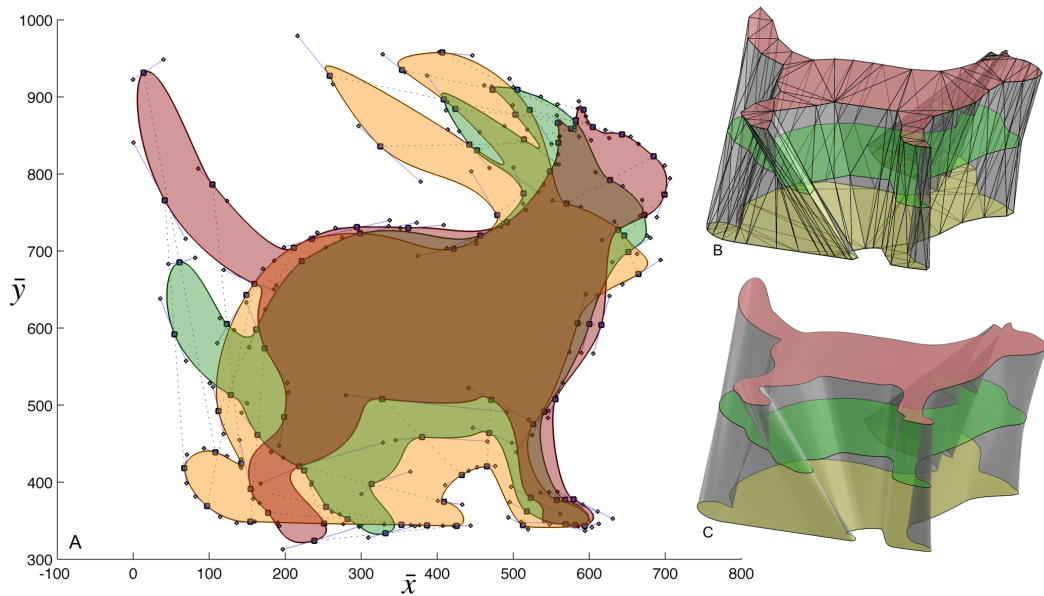


Figure S1. Polyhedron creation process. Two shapes, the red cat and the yellow rabbit, are defined by polygons in the drawing plane ( $\bar{x}$ ,  $\bar{y}$ ) at two different positions along  $\bar{z}$ . The position of each node of the Bezier curve defining the cat and rabbit are interpolated at an intermediate  $\bar{z}$  position to yield the green shape. **A)** Square and circles are nodes of the bezier curves. Nodes of the green shape result from the interpolation between the red and the yellow shapes. **B)** Wireframe representation of a low resolution mesh. **C)** high resolution mesh.

The SVG standard `<path>` object describes a cubic multi-segment Bezier curve, with four points associated with each segment defining their respective shape. Each of these points defining the path segment is interpolated along the third dimension to create interpolated Bezier curves (Fig. ??). Our approach is similar to the so-called shape interpolation technique used in computer animation (Parke, 1972).

The triangulation algorithm works as follows. Across slices, one triangle connects two points with the same index and one neighbor on either slice. For the first and last slice, polygons are triangulated using MATLAB's `De1aunay` function. If the polygon is not convex, then triangles outside of the polygon are excluded by performing a point-in-polygon test for the center of triangles (Fig. ??b and c). For the point-in-polygon tests, we use the function `InPolygon` by Redish and Jaquenot (2008). In general, this triangulation method can be used to connect polyhedrons across planes with arbitrary orientations. However, for simplicity, in `geomIO`, we impose the restriction that a given volume must be drawn from parallel planes. When objects are created by interpreting data, it is usually necessary to project data on these planes before drawing the objects. We find that this approach ensures mesh quality and is the easiest in terms of drawing, although this restriction could be lifted off in a future update.

## S4. Material phase assignment

In numerical models, material properties are defined on vertices, which can be Lagrangian (as in marker-in-cells and body fitted methods) or Eulerian (as in level set methods). In most geodynamic models, basic material properties (e.g., density, plastic, elastic and viscous flow law parameters, as well as thermal properties and others) are defined by material phases, where each phase represents a different rock type. Phases are considered to be discrete, i.e., a vertex is either of phase one or two but not a mixture. We, therefore, define the initial

geometry by setting up a set of polyhedrons inside of which the phase takes a constant value.

We assign properties by performing a point-in-polygon test. This approach is easier to program and less computationally expensive than the point-in-polyhedron test. To perform the point-in-polygon test in 3D, we cut polyhedrons along each plane of vertices and store the polygon that describes the intersection between the polyhedron and the cutting plane. The slicing consists of calculating the intersection between the slicing plane and each of the triangles composing a given volume. For this action we use the function `intersectPlaneSurf` by Ozturk (2014). The set of polygon slices for each of the polyhedrons of a given model are saved in a 'Polygon' file to be read by thermomechanical modeling software. An implementation of the point-in-polygon function is given in the folder `supporting_src` as a C mex file (MATLAB) and a PETSc C implementation.

To deal with overlapping polyhedrons, they must be handled sequentially when assigning a material phase. For example, let's consider two overlapping polyhedrons A and B, with B written after A in the polygon file. Using the algorithm described in the next section, we first assign the material phase A to vertices within polygon A. We then assign material phase B to all vertices within polygon B including the ones which were previously assigned with phase A. Therefore, the order in which polyhedrons are stored in the file matters. In 2D, by default, polygons are read in the order they are stored in the SVG file, which corresponds to the drawing order from bottom to top. In 2D and 3D, the user can also enforce the order in which polyhedrons are read and written by specifying `opt.pathNames` and their order. For example, specifying `opt.pathNames=['volumeB', 'volumeA']`, ensures that the data of polyhedron A will be written after the one of polyhedron B, and therefore phase A will overwrite phase B. Besides, the `volumes` objects have a `type` property which is zero by default that ensures the behavior described above. Alternatively, the `type` can be set to one, resulting in incremental behavior. For example, the portion of a polyhedron associated with phase A overlapping with another phase B polyhedron is assigned a new phase equal to the sum of A and B.

## S5. The Polygon file format

In case of regular markers grids, one slice is created for each grid plane along the orthogonal grid directions, meaning the polygon files are created for a given resolution in the normal direction. When the resolution in this direction is changed, the polygon file must be recreated. However, changing the resolution in the directions spanning the slicing plane does not require creating a new file. The polygon files are binary files, where the header is composed as follows:

```
nPH, maxPolygonPerPolyhedron, maxPolygonLenth
```

The header contains information used for memory assignment followed by `nPH` polyhedrons segments

```
normal, phase, type, nPolygon, listIndex, listPolygonLength, listCoordVertices
```

The description of each element of the file format is given in Table ?? and an algorithm for reading this file format is given below as pseudocode. The algorithm works efficiently in parallel when markers are stored in distributed memory.

```
Read file header
Allocate memory using header info
Continue reading file
for each Polyhedron:
    get normal, phase, type, nPolygon
```

Table S2. Items of the polygon file format

Label	Description
nPH	number of polyhedrons
maxPolygonPerPolyhedron	maximum number of polygons per polyhedron
maxPolygonLenth	maximum length of a polygon's coordinate list
normal	normal direction to the plane in which the polygons are defined (0,1 or 2)
phase	phase index for this volume
type	if 0: assign this phase index to the particle; if 1: increment this phase index to the particle's phase
nPolygon	number of polygons (i.e., slices) composing this polyhedron
listIndex	list of the indexes of the planes which contain the polygons (length=nPolygon)
listPolygonLength	list of the lengths of all the polygons defining this volume (length=nPolygon)
listCoordVertices	list of x,y coord. (in the plane) of all vertices of all polygons in this volume (length=2*nPolygon*sum(listPolygonLength))

```

for each Polygon in this Polyhedron // i.e., for each plane in the normal direction
  get the plane index
  get Polygon.XY = listCoordVertices // get the coordinate list of all the vertices
  get Marker.XY // get the marker coordinate list
  [IN] = inpoly(Part.XY, Polygon.XY)
  // inpoly is included in geomIO
  // (in C or mex)
  if type == 0
    Part.Phase[IN] = Phase
  else if type == 1
    Part.Phase[IN] += Phase
  end
end
end
end

```

## S6. Temperature assignment

### Simple vertical temperature profile

The initial conditions of geodynamic numerical simulations are described by phase geometry and initial temperature distribution. In geomIO, one can set the temperature based on an SVG file where the drawing plane represents the horizontal plane of the model space. Temperature is computed according to a 1D function in the vertical direction (eq. ??). Two types of functions are available by default: piecewise linear or a half-space cooling model for a given lithospheric thermal age. The half-space cooling model is given as (e.g., Turcotte and Schubert, 2014):

$$T(D) = T_m \operatorname{erf}\left(\frac{D}{2\sqrt{\kappa t}}\right), \quad (2)$$

where  $T(D)$  is the temperature at a given depth  $D$ ,  $T_m$  is the temperature of the mantle (1573 K by default in geomIO), erf is the error function,  $\kappa$  is the diffusivity and  $t$  is the age of the plate. This function is accessible through the function `initTemp` which takes a reference SVG layer as an argument (through `PathCoord`) and temperature profile information, as well as a 3D temperature grid. The function reads the layer and assigns a given temperature profile to each polygon found on this layer. The function `initTemp` implements these algorithms and applies in function of the polygons drawn at the surface of the model. The

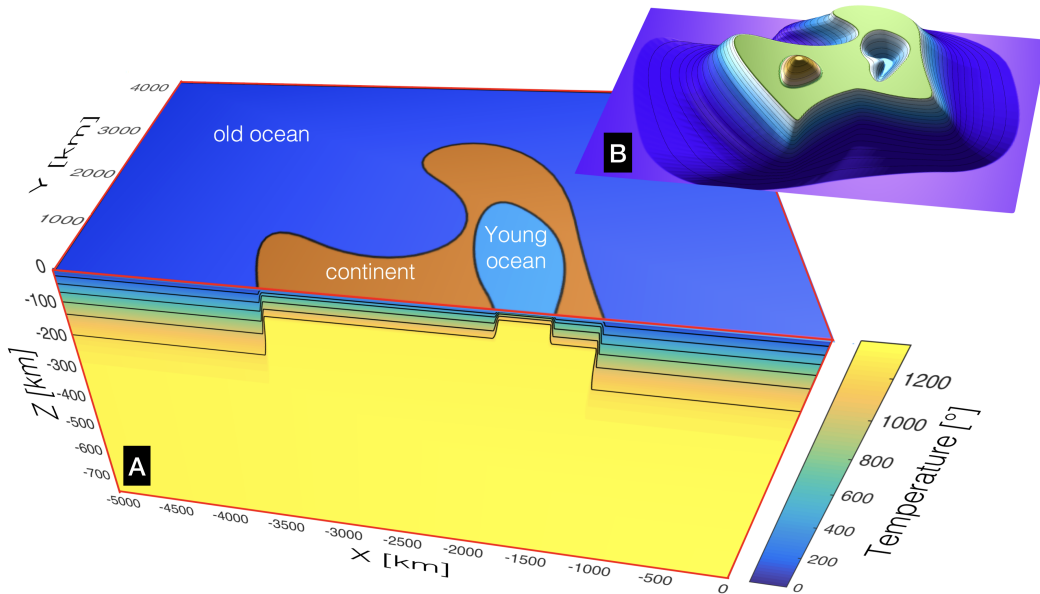


Figure S2. A) Example of initial temperature distribution. On the upper surface of the cube, the phase geometry is represented. On the side, the initial temperature is shown. The temperature below the oceans is assigned following a half-space cooling model with 80 Myrs and 5 Myrs for the *old ocean* and *young ocean*, respectively. The temperature below the *continent* is piecewise linear with gradients of 25 K/km up to 30 km depth, then 1 K/km up to 95 km depth, below which the temperature is constant. B) 3D rendering of the topography of the model

example `Example3D_Geodynamics` shows the usage of this function with a non-planar surface topography (Fig. S2).

### Complex 3D temperature distribution

One may need to construct a numerical model whose geometry incorporates an already subducting oceanic slab. The geometry of subducting slabs is non-cylindrical and can be overturned such that it is non-trivial to specify the temperature distribution in and around it (e.g., Jadamec and Billen, 2012). Our strategy involves a few assumptions and consists of (1) a 3D representation of the slab surface, which is often well known through earthquake distribution and is available for many regions (Hayes et al., 2012), and (2) 1D temperature profiles. For oceanic lithosphere, 1D temperature profiles such as half-space cooling are defined as a function of depth and age. Combined with age maps (Müller et al., 2008), this can be a first approximation of the 3D temperature distribution. In our approximation, the temperature of the slab is computed as a function of distance  $d$  from a point within the slab to the closest point on the slab surface. Thus, for the 1D representation, distance  $d$  is equivalent to depth  $D$  in eq. 2. We represent the temperature field on a regular 3D grid. To compute  $d$  efficiently, we employ the algorithm proposed by Velić et al. (2009) to construct an approximate discrete Voronoi diagram. The Voronoi diagram attributes the closest slab point to every grid point.

Attributing a half-space cooling model in the mantle above the slab is undesirable. Therefore, we test whether the points of the grid are above or below the slab top surface. This condition is tested by computing the dot product  $v_p \cdot v_n$ , where, for a given grid point,  $v_p$  is the vector from the closest point of the slab surface mesh to this grid point; and  $v_n$  is the vector normal to the slab surface at the closest mesh point. The slab surface mesh is constructed such that all  $v_n$  point either towards above or below the slab.

This function is accessible via the function `getDistanceFromSlab`. The function re-

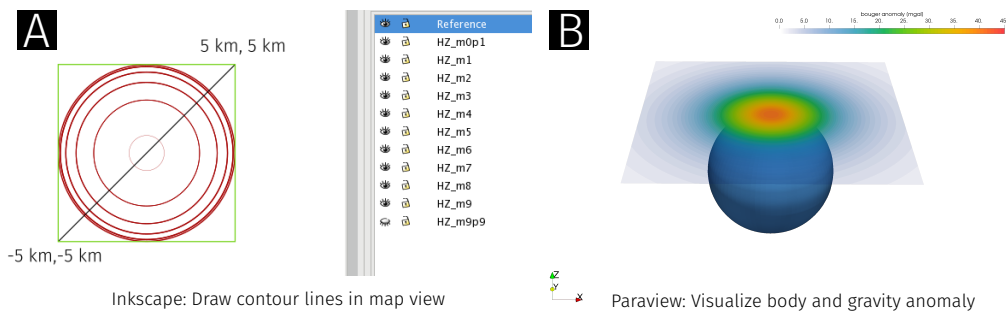


Figure S3. Example of 3D gravity computation with geomIO. **A)** Horizontal contour lines of 3D bodies in Inkscape. The contour lines can either be directly used with Talwani’s method (Talwani and Ewing, 1960) to compute the gravity anomaly of the body (**B)**. Or, the drawing can be performed on one of the vertical ortho views, in which case a 3D volume is created and cut in horizontal laminae with the geomIO engine, before being passed to the gravity computation.

turns the distance to the closest slab surface mesh point for the condition that the grid point is below the slab surface. The example `Example3D_Slab_Temperature` in the `Tutorials` folder gives an example of the usage of this function and generates the temperature distribution shown in Fig. 6.

### Temperature file format

The initial temperature distribution is stored as a 3D matrix of arbitrary size. For example, in LaMEM, a linear interpolation is performed between the initial temperature grid stored in the file and the grid used in the numerical simulations. The stored temperature grid is equally spaced and the information is assumed to be stored at the center of the cells. The file contains a header with  $nx$ ,  $ny$ ,  $nz$ , the size of the grid in each direction and followed by the temperature data in the order going through  $x$ , then  $y$ , then  $z$ .

### Topography file format

An initial topography grid can be constructed from the polyhedrons by calling the function `initTopo`, which stores a 2D topography array. `initTopo` writes a file containing a header with  $nx$ ,  $ny$ , the size of the grid in each direction, followed by the topography data in the order going through  $x$ , then  $y$ . The example `Example3D_Geodynamics` shows the usage of the function (Fig. S2B). The topography grid can be used in two ways within thermomechanical codes. If phases are assigned to markers, all markers above the topography should be deleted or assigned some neutral phase (e.g., sticky air). Besides, the grid can also be used to define the top surface of the mesh (FEM) or an internal boundary.

### Endianness

In geomIO all binary files are written using the `PetscBinaryWrite` function (part of the PETSc library, Balay et al., 2018). Therefore binary files always employ big-endian and are independent of the hardware architecture.

## S7. Gravity computation

In gravity modeling, polygonal shapes are used since the late 1950s to perform forward modeling of gravity anomalies in 2D (Talwani et al., 1959). Talwani and Ewing (1960) extended this method to three dimensions, which can be easily adapted to polyhedrons that are

constructed with geomIO because it suites well to the fundamental idea of the geomIO toolbox. 3D bodies are constructed from polygons on 2D cross-sections, which coincides with Talwani's method of gravity computation, where 3D bodies are discretized with horizontal laminae of finite thickness. Fig. ?? provides an example of a spherical anomaly (Fig. ??A) constructed in Inkscape by drawing contour lines on several horizontal sections. The workflow pipeline is not different from other examples. As usual, a PathCoord structure and a Volumes object are created. Both of them can be used by geomIO to compute the gravity anomaly. The associated geomIO function polygrav3D either accepts PathCoord's contour lines or horizontal polygon slices from Volumes. The second option is more general and allows the user to draw the 3D volume from any of the three ortho views. Using geomIO for gravity modeling offers a couple of advantages. It is well known that models of gravity anomalies are ambiguous and good initial estimates are of great value to prevent non-physical solutions. With geomIO, one can quickly create different initial guesses and test whether these models make sense in terms of gravity anomaly, provided the respective gravity data is available.